

Received May 5, 2020, accepted May 25, 2020, date of publication May 28, 2020, date of current version June 9, 2020.

Digital Object Identifier 10.1109/ACCESS.2020.2998131

Dual-Band Focused Transmitarray Antenna for Microwave Measurements

ZHENG ZHANG¹, XIAOPING LI, CHAO SUN², YANMING LIU¹,
AND GAO HAN¹

¹Key Laboratory of Information and Structure Efficiency in Extreme Environment, Ministry of Education of China, Xidian University, Xi'an 710071, China
²School of Aerospace Science and Technology, Xidian University, Xi'an 710071, China

Corresponding author: Zheng Zhang (zhang_xidianer2018@163.com)

This work was supported in part by the Chinese National Natural Science Foundation under Grant 61627901 and Grant 61801343.

ABSTRACT A dual-band focused transmitarray antenna designed by using frequency selective surfaces (FSS) technique is proposed in this paper. Compared with the traditional transmitarray antenna, the proposed antenna has advantages of good ability to focus electromagnetic wave in the dual-band, high resistant of poor measurement environment and easy to process. The transmitarray consists of four identical metal phase shift layers, each of which is separated by an air gap. The elements distributed on metal layer are composed of a I-shaped slot at the center and four L-shaped slots with central symmetry. The change of I-shaped slot length affects the change of phase in low frequency band and the change of L-shaped slot length affects the change of phase in high frequency band. The mutual coupling between the two kinds of slots can be neglected. The proposed antenna consisting of a transmitarray and a feed has been analysed, simulated, and measured. The results show that the average focal spot diameter (SD) is 35.2 mm at 12 GHz and 24.5 mm at 18 GHz, and the dual-band focused transmitarray antenna can operate in two frequency bands 11.8-12.2 and 17.8-18.1 GHz. Simulated and measured results show that the proposed antenna has good concordance, making it possible for various microwave measurements.

INDEX TERMS Focused, all metal elements, dual-band, transmitarray antenna, frequency selective surfaces (FSS).

I. INTRODUCTION

Recently, focused antennas have attracted wide attention in microwave measurement systems. Because of its good directivity, it can concentrate electromagnetic energy in a small area [1]. The energy of electromagnetic wave focused on a certain point of the target can be used to diagnose the electromagnetic parameters, such as measuring the electron density in the plasma.

The traditional dielectric lens is usually adopted in the design of the focused antenna, and Teflon is mostly used as the lens material. The ray-optics theory is used to write an equation describing the lens profile, that is, the optical path from the feed to each point on the lens surface must be equal [2]–[5]. For example, in [2], a focused lens horn antenna with different spread angle has been studied. When the spread angle of horn is 30°, the focal spot diameter of the antenna is less than 2 times the wavelength. In [3], a focused lens conical

horn antenna loaded with dielectric has been designed. The antenna consists of a horn feed and a lens loaded with uniform dielectric. The antenna has a wide bandwidth, but its sheer weight and processing complexity severely restrict the application for some circumstances. Compared with the traditional lens antenna, the transmitarray antenna based on frequency selective surfaces (FSS) structures has similar performance and smaller size, which makes it possible to design a focused antenna using FSS structures. In [6], a 2-bit-design method is used to reduce the number of layers in the structure design. When dielectric substrate is used in the transmitarray lens, a 25 mm quasi-circular spot has been obtained while the value of the secondary lobes is lower than -15 dB. In [7], a transmitarray antenna with no dielectric substrate is proposed. When the transmitarray works well, the loss of air is much lower than that of the dielectric substrate, and the weight of the antenna is greatly reduced by using the metallic layers. The results show a focused radiation beam can be achieved, but it can only converge the spherical incident wave transform into the plane wave on the other side, which cannot meet the

The associate editor coordinating the review of this manuscript and approving it for publication was Chow-Yen-Desmond Sim¹.

required requirements. The transmitarray lens with simpler structure can also be found in [8]–[14].

At the same time, the operating frequency band is an important parameter to be considered in the design of transmitarray antenna. It is a challenging task to achieve a 360° of phase shift range in different frequency bands while the transmission magnitude better than −3 dB. Although dual-band reflectarrays have been widely studied [15]–[17], there is little literature on the design of dual-band transmitarrays [18]–[22]. The principle of dual-band transmitarray is similar to that of traditional transmitarray, that is, dual-band transmitarray can operate normally in both bands without changing the entire structure. Therefore, a dual-band transmitarray can be thought of as the integration of two traditional transmitarrays in two different operating frequency bands. In [18], a dual-band three-layer metallic slot transmitarray for 11/12.5 GHz bands is proposed. In [19], the dual-band element consists of two kinds of rectangular slots, in which the center larger slot and the two outer smaller slots control the transmission phase independently at 12 and 18 GHz respectively, and the mutual coupling between them can be neglected. In [20], [21], the transmitarray antennas are composed of two different interlaced slots for dual-band operation. Hasani *et al.* [22] showed a dual-band circularly polarized transmitarray antenna for satellite communications, which can achieve beam scanning at both frequency bands. A typical transmitarray either converges the electromagnetic wave in only one frequency band, or only increases the gain in different frequency bands. Therefore, the dual-band focused transmitarray antenna now is in urgent need.

In this paper, a dual-band focused transmitarray antenna using all-metal slot elements is presented. The designed transmitarray antenna consists of a quad-layer metallic array and a pyramidal horn. A 360° transmission phase response can be obtained by changing different kinds of slots independently in both low and high frequency bands respectively. The simulated and measured results demonstrate that the proposed antenna has excellent electromagnetic wave convergence. The maximum electric field strength is obtained at the distance of $6.47\lambda_{\text{lower}}$ from the array aperture at 12GHz and at the distance of $9.78\lambda_{\text{higher}}$ from the array aperture at 18GHz. Besides, through reasonably arranging the all-metal slot elements, the focal spot diameter of 35.2mm ($1.41\lambda_{\text{lower}}$) at 12GHz and 24.5mm ($1.47\lambda_{\text{higher}}$) at 18GHz can be achieved from the measured results. At the same time, the dual-band focused transmitarray antenna can operate in two frequency bands 11.8-12.2 and 17.8-18.1 GHz.

II. ANTENNA DESIGN

The geometry of the proposed dual-band focused transmitarray antenna is illustrated in Fig. 1.

Basically, the antenna consists of two parts, a horn feed and a focused transmitarray. The focused transmitarray adopts a quad-metallic-layer structure composed of all-metal slot elements, and there is an air gap between each two layers, and each layer has 256 (16×16) elements. The design of the

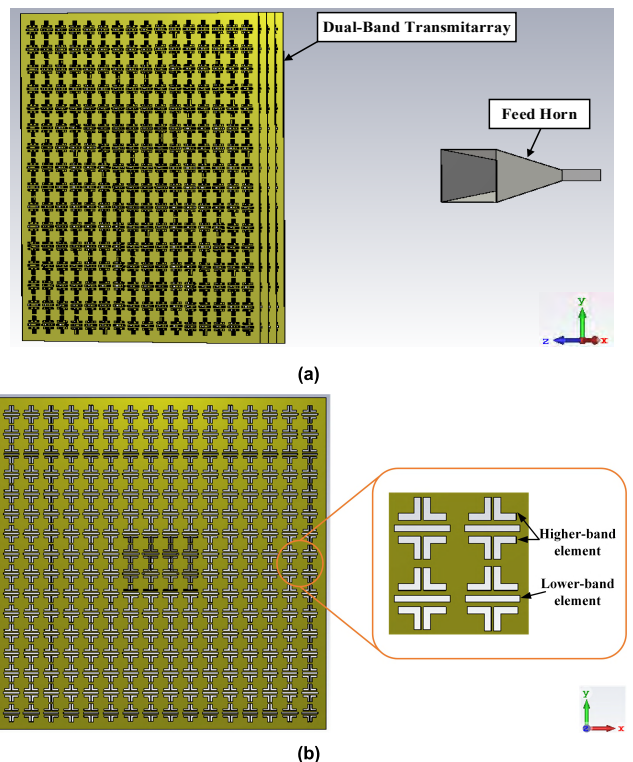


FIGURE 1. Configuration of the proposed antenna. (a) 3-D view. (b) Top view.

antenna is divided into two parts. Section A introduces the design of the dual-band element and Section B is the design of the focused transmitarray antenna.

A. DUAL-BAND ELEMENT DESIGN

An FSS is a periodic array structure that can form a band-stop characteristic or a band-pass characteristic at a specific operating frequency. Because a focused transmitarray antenna is proposed in this paper, the first problem to be solved is the design of elements with band-pass filter characteristics.

Two different structures of band-pass all-metal slot elements are designed. The slot elements are all made of a quad-metallic-layer structure with an air gap between every two layers, and the period of the both slot elements is the same. TM-mode excitation is very effective since the proposed element is linearly polarized. The responses of transmission and reflection coefficients of the I-shaped slot element and the L-shaped slot element are shown in Fig. 2. It can be seen that a total transmission occurs at 12 GHz when the I-shaped element is used, and at 18 GHz when the L-shaped element is used. When total transmission occurs, strong inductive electric fields are generated on the two different elements respectively. This provides a powerful help for the design of dual-band elements.

Through the above analysis, a dual-band slot element formed by combining the I-shaped slot with the L-shaped slot are shown in Fig. 3. According to the operation frequency of the element, the periodicity of the dual-band slot element is $p = 15\text{mm}$, the air gap height between each two layers is

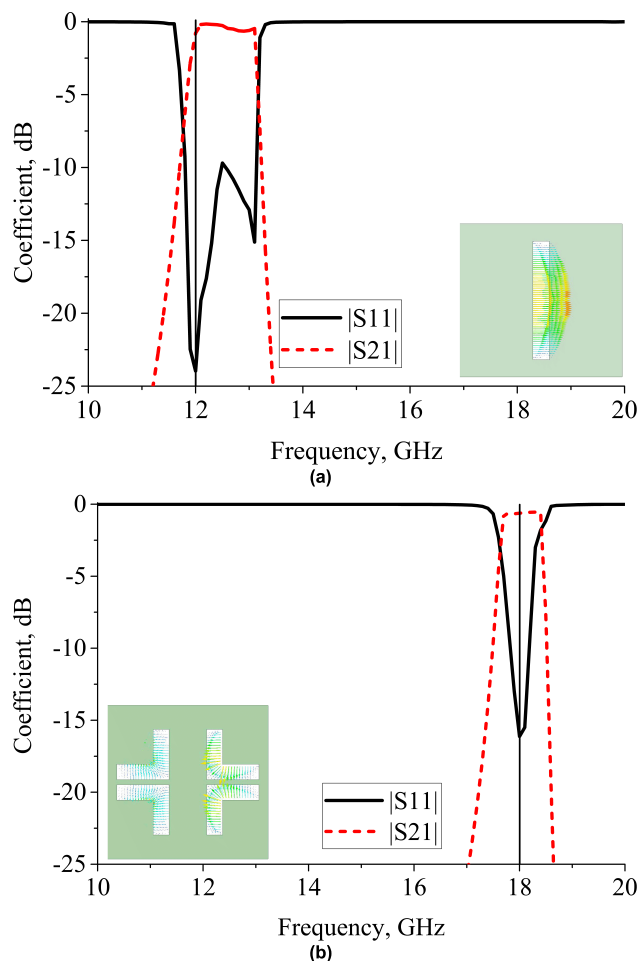


FIGURE 2. Transmission and reflection coefficients of elements. (a) The I-shaped slot element. (b) The L-shaped slot element.

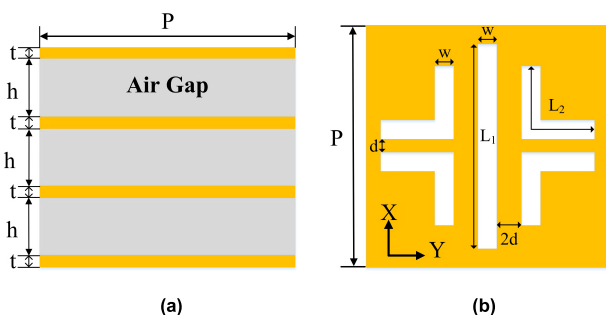


FIGURE 3. Schematic of the dual-band slot element. (a) Lateral view. (b) Top view.

h, the width of the slots are recorded as w , and the length of the I-shaped slot and the L-shaped slot are L_1 and L_2 respectively, the spacing between adjacent L-shaped slots is d , the distance between the I-shaped slot and the L-shaped slot is $2d$. Because the dual-band slot element is made of all metal without any substrate, it is necessary to strike a compromise between better performance and mechanical strength. In this paper, the thickness $t = 0.3$ mm is chosen.

The dual-band slot element needs to have relevant electromagnetic responses in different frequency bands. When

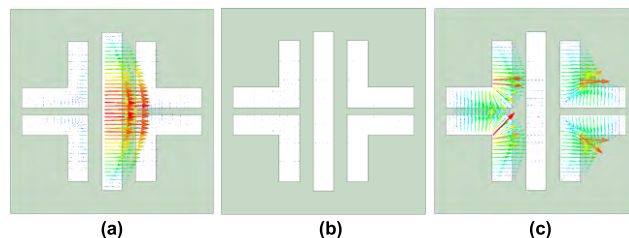


FIGURE 4. Induced electric field of the dual-band slot element at frequencies of (a) 12 GHz. (b) 15 GHz. (c) 18 GHz.

TABLE 1. Parameters of dual-band slot element.

Parameter	p	L_1	L_2	w
Value(mm)	15	11.50~12.61	9.70~10.34	1.5
Parameter	d	h	t	
Value(mm)	0.5	5.2	0.3	

electromagnetic waves of different frequencies are irradiated on this dual-band slot element, the induced electric field generated by the element can be obtained from Fig. 4. The I-shaped slot produces a strong induced electric field at 12 GHz, the L-shaped slot produces a strong induced electric field at 18 GHz, while at 15 GHz, there is essentially no induced electric field. It follows that the dual-band slot element can be well equivalent to a dual-band filter. Table 1 shows the final parameters of the proposed element optimized in the electromagnetic simulation software.

The variation of the transmission phase and amplitude can be obtained by changing the value of L_1 or L_2 at different frequencies. Floquet port method is used in this simulation, and the related transmission responses is shown in Fig. 5. At 12 GHz, as L_1 increases from 11.50 mm to 12.61 mm, the variation of the transmission phase achieves a 360° phase shift, and the magnitude of S_{21} is better than -2.8 dB. Similarly, it can be seen that when L_2 changes from 9.70 mm to 10.34 mm, the phase achieved a 360° range variation at 18 GHz, while the amplitude of S_{21} is better than -2.6 dB. The proposed element can obtain the desired phase shift in two different frequency bands by changing the lengths of L_1 and L_2 , respectively.

In the design of dual-band slot element, the mutual coupling between different slots is also a problem worthy of further research. In other words, the change of I-shaped slot should only affects the phase shift of low frequency band, while the change of L-shaped slot should only affects the phase shift of high frequency band.

On the one hand, the distribution of induced electric fields at different frequencies shows that there is basically no mutual coupling between different slots, as shown in Fig. 4. On the other hand, the effect of changing the length of I-shaped slot at 18 GHz on the transmission parameters and changing the length of L-shaped slot at 12 GHz on the transmission parameters, as shown in Fig. 6. It can be seen that with the variation of L_1 or L_2 , the magnitude and phase of S_{21} have only a slightly fluctuate. Generally speaking, the proposed element has excellent isolation.

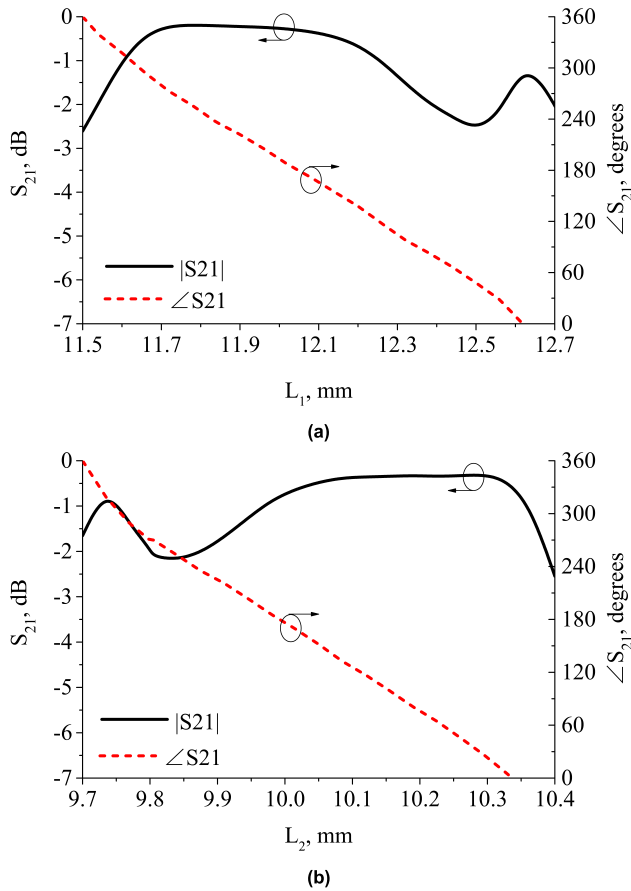


FIGURE 5. Transmission coefficients of the dual-band slot element (a) Varied slot length L_1 at 12GHz. (b) Varied slots length L_2 at 18GHz.

In numerical analysis, the horn feed is generally substituted by a plane wave. Thus, it is of great significance to analysis the influence of different oblique incidences on the transmission coefficients of the dual-band slot element, and the results are shown in Fig. 7. It is noticeable that when the angle of oblique incidence (ϕ from 0° to 90°) is less than 15° , the transmission magnitude and phase have small fluctuations in the dual-band. However, when the oblique incidence angle continues to increase, the transmission coefficients become significantly worse. This is because when the incident wave has been illuminated on the surface of the element at a certain angle, there will be a dislocation between the two adjacent layers, which leads to different values of the slot length or width, and then has a negative impact on the transmission coefficients.

B. FOCUSED TRANSMITARRAY ANTENNA DESIGN

Fig. 8 shows a schematic diagram of an electromagnetic wave propagation path on the focused transmitarray. Since the entire transmitarray operates in a dual-band, the phase delay of adjacent elements is compensated by designing the transmission phase of each dual-band slot elements at different frequencies to achieve the purpose of converging electromagnetic wave. If the coordinates of any element on

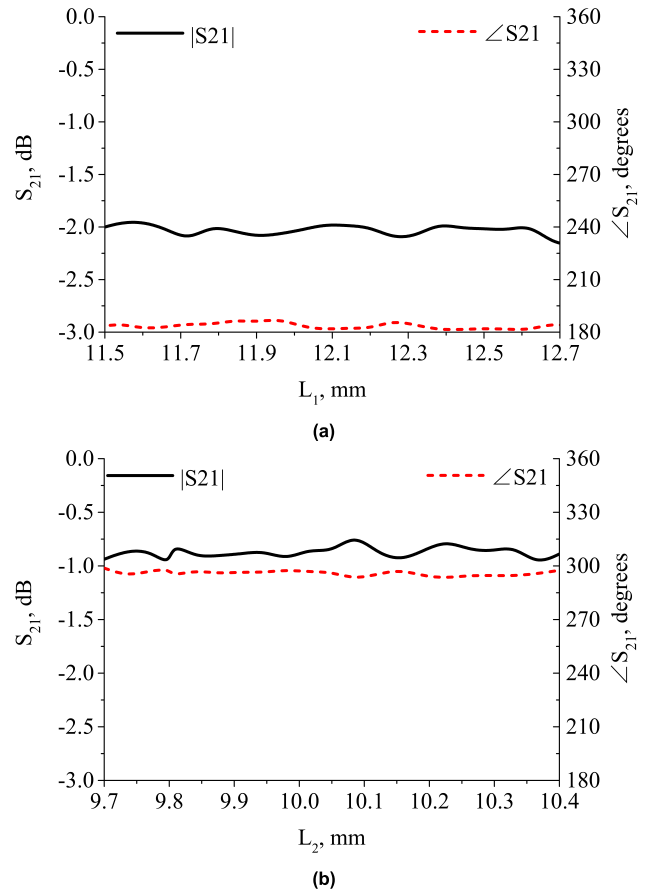


FIGURE 6. Effect of the mutual coupling on the transmission coefficients of the dual-band slot element. (a) Transmission parameters at 18GHz for varied slot length L_1 when L_2 is fixed to 10mm. (b) Transmission parameters at 12GHz for varied slot L_2 when L_1 is fixed to 11.9mm.

the focused transmitarray can be expressed as (x_{ij}, y_{ij}) and the focal length is recorded as F_t , the transmission phase difference $\Delta\phi_i$ for the i th element is shown in equation (1).

$$\Delta\phi_i = 2 \cdot k \cdot (\sqrt{R_i^2 + F_t^2} - F_t) \tag{1}$$

$$R_i = \sqrt{x_{ij}^2 + y_{ij}^2} \tag{2}$$

where k is the propagation constant, and equation (2) denotes the distance from the center of the focused transmitarray to any element. It can be observed that the required phase shift is greater than 360° if the emitted electromagnetic wave is focused at a focal length form the array aperture. Considering the periodicity of the phase, the transmission phase of each element on the transmitarray can be obtained quickly according to equation (1) and equation (2) and using MATLAB programming. The phase distributions at 12 GHz and 18 GHz are shown in Fig. 9(a) and (b), respectively.

III. MEASURED RESULTS AND DISCUSSION

For the feed antenna, a Ku-band pyramidal horn with gain of 15.5 dBi at 12 GHz and 18.3 dBi at 18 GHz is selected. The diameter of the overall transmitarray is $D = 250$ mm

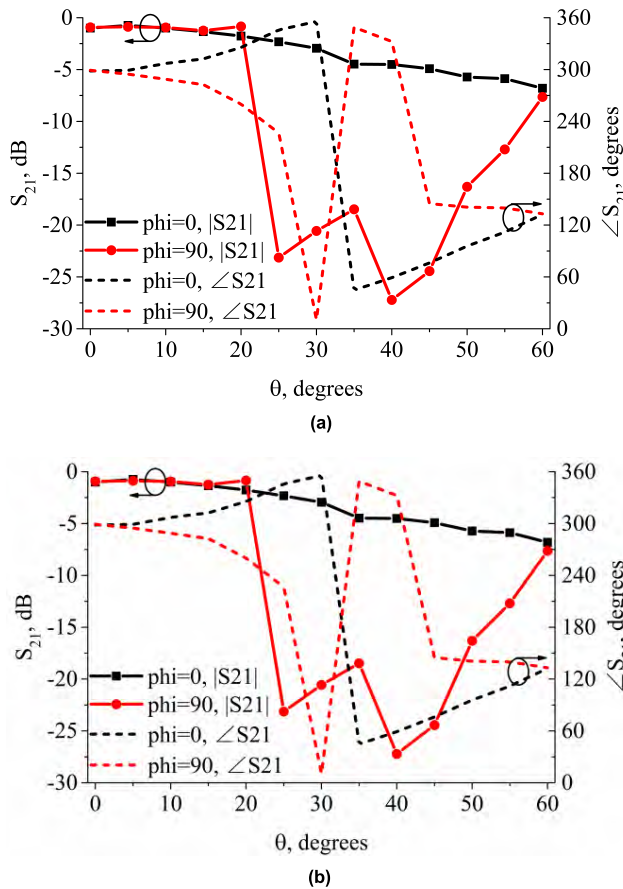


FIGURE 7. The transmission coefficients (magnitude and phase) of the element for various incidence angles at dual-band. (a) At 12GHz. (b) At 18GHz.

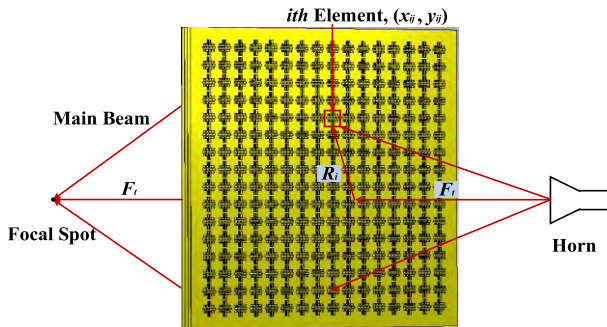


FIGURE 8. Schematic of focused transmitarray antenna for phase analysis.

($10\lambda_{\text{lower}}$ at 12 GHz and $15\lambda_{\text{higher}}$ at 18 GHz) and the focal length to diameter ratio is tagged by F_t/D as 0.8. The three-dimensional electromagnetic simulation software CST has been used to simulate the relative results of the transmitarray antenna. Fig. 10 shows the simulation results of the instantaneous electric strength of the focused transmitarray antenna at 12 GHz and 18 GHz. According to the scale in the fig. 10, the focused transmitarray antenna can focus at about 370 mm at 12 GHz, and the focused transmitarray antenna can focus at about 380 mm at 18 GHz. It can also be seen that there is some diffraction at 18 GHz, which is because when the focal

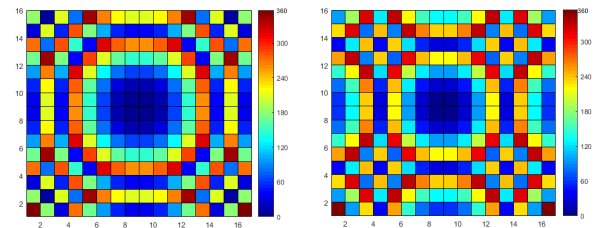


FIGURE 9. Transmission phase distribution of elements on the antenna aperture at (a) 12GHz and (b) 18GHz.

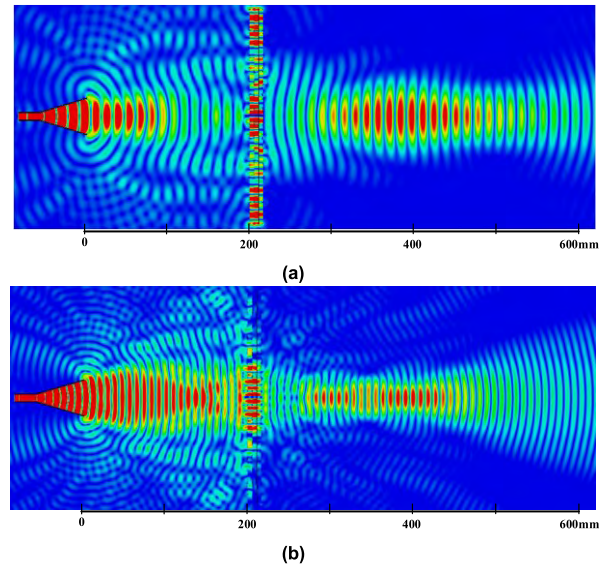


FIGURE 10. Focused transmitarray antenna electric intensity instantaneous value at (a) 12GHz and (b) 18GHz.

length is fixed, the transmitarray antenna needs to focus on a larger electronic size, that makes it difficult compared to the case of 12 GHz, and oblique incidence also caused a certain impact at the same time, so the performance of converging electromagnetic wave is better in the low frequency band.

Focal plane is the plane that passes through the maximum value of the electric field strength and is perpendicular to the z-axis, it's electric field intensity effective value at different frequencies are shown in Fig. 11. It can be seen that the proposed antenna has obvious convergence effect in the focal plane, and the focal spots of the two frequency bands are elliptical. However, the feed horn antenna has almost no convergence.

According to the simulation model, the focused transmitarray antenna has been manufactured and measured. Fig. 12 shows the measurement environment of the focused transmitarray antenna, it can be seen that the quad-metallic-layer structures fixed by twenty-eight plastic pins, and these pins have hardly influence on the results. The phase center of the feed antenna is located at a focal length from the center of the array aperture at two different frequency bands, by precisely and slightly moving the feed antenna. In order to verify the dual-band characteristics, the distance between the transmitarray and the feed antenna and the polarization

TABLE 2. Simulated and measured focal spot diameter.

Frequency (GHz)		12GHz		18GHz	
Focal Spot Diameter (mm)	E-Plane	Sim.	41.7	Sim.	19.9
		Meas.	43.4	Meas.	20.0
	H-Plane	Sim.	24.3	Sim.	24.7
		Meas.	27.0	Meas.	29.0

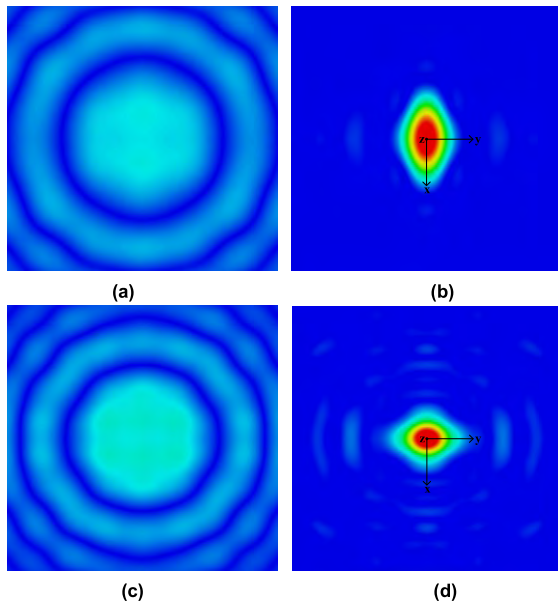


FIGURE 11. The focal plane electric field intensity of two kinds of antenna at different frequencies: (a) feed horn antenna at 12 GHz; (b) focused transmitarray antenna at 12 GHz; (c) feed horn antenna at 18 GHz; (d) focused transmitarray antenna at 18 GHz.

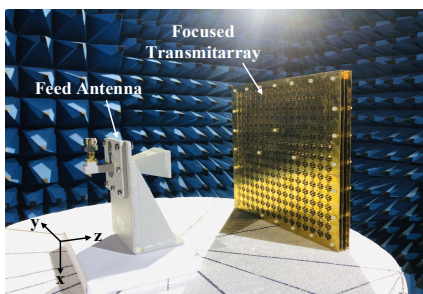


FIGURE 12. Focused transmitarray antenna setup and the measurement environment.

remain unchanged when the feed frequency rises from the low frequency (12GHz) to the high frequency (18GHz). Anritsu high performance network analyser MS4640B Series is used to measure the electric field intensity distribution of the proposed antenna, and the relevant results are shown below.

It is observed from Fig. 13 that the focused transmitarray antenna could obtain the maximum value of the electric field strength at a point with $6.47\lambda_{\text{lower}}$ distance from the array aperture at 12 GHz and at a point with $9.78\lambda_{\text{higher}}$ distance from the array aperture at 18 GHz. There is a another peak

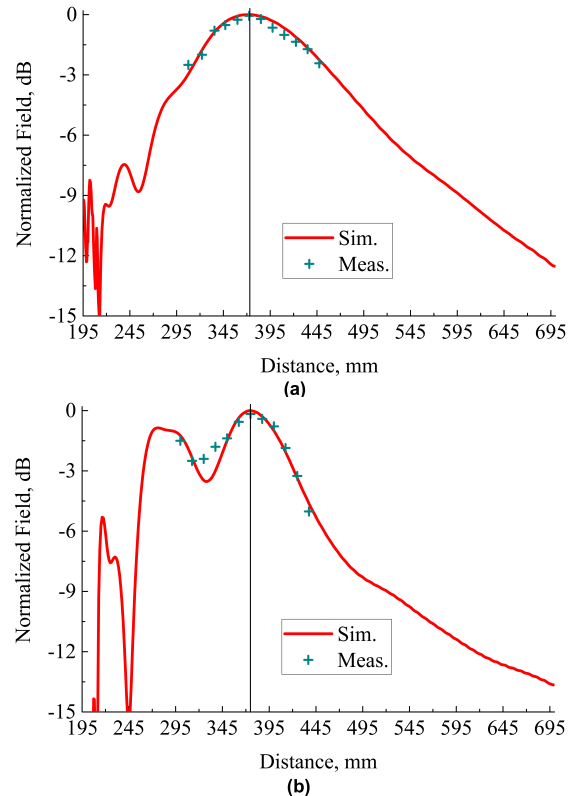


FIGURE 13. Measured and simulated electric field strength distribution along the z-axis at (a) 12GHz and (b) 18GHz.

value of electric field strength at about 275 mm at 18 GHz, which can also be explained in Figure 10 (b). The existence of this value has little effect on the trend of the overall electric field strength distribution. In the dual-band, the measurement results are slightly lower than the simulated results. The difference may be attributed to errors in processing accuracy and intrinsic noises in the measurement environment.

Fig. 14 shows the simulated and measured normalization radiation patterns of the focal plane at 12 and 18 GHz, which are in good agreement compared to the simulated results. The focal spot diameter (SD) is a key parameter of the focused antenna, and the SD can be obtained by calculating the distance of the electric field strength decreasing by 3 dB. It can be seen that the SDs of the measurement is slightly different from that of the simulation. For ease of analysis, the results of simulation and measurement of focal spot diameters at both frequencies are tabulated in Table 2.

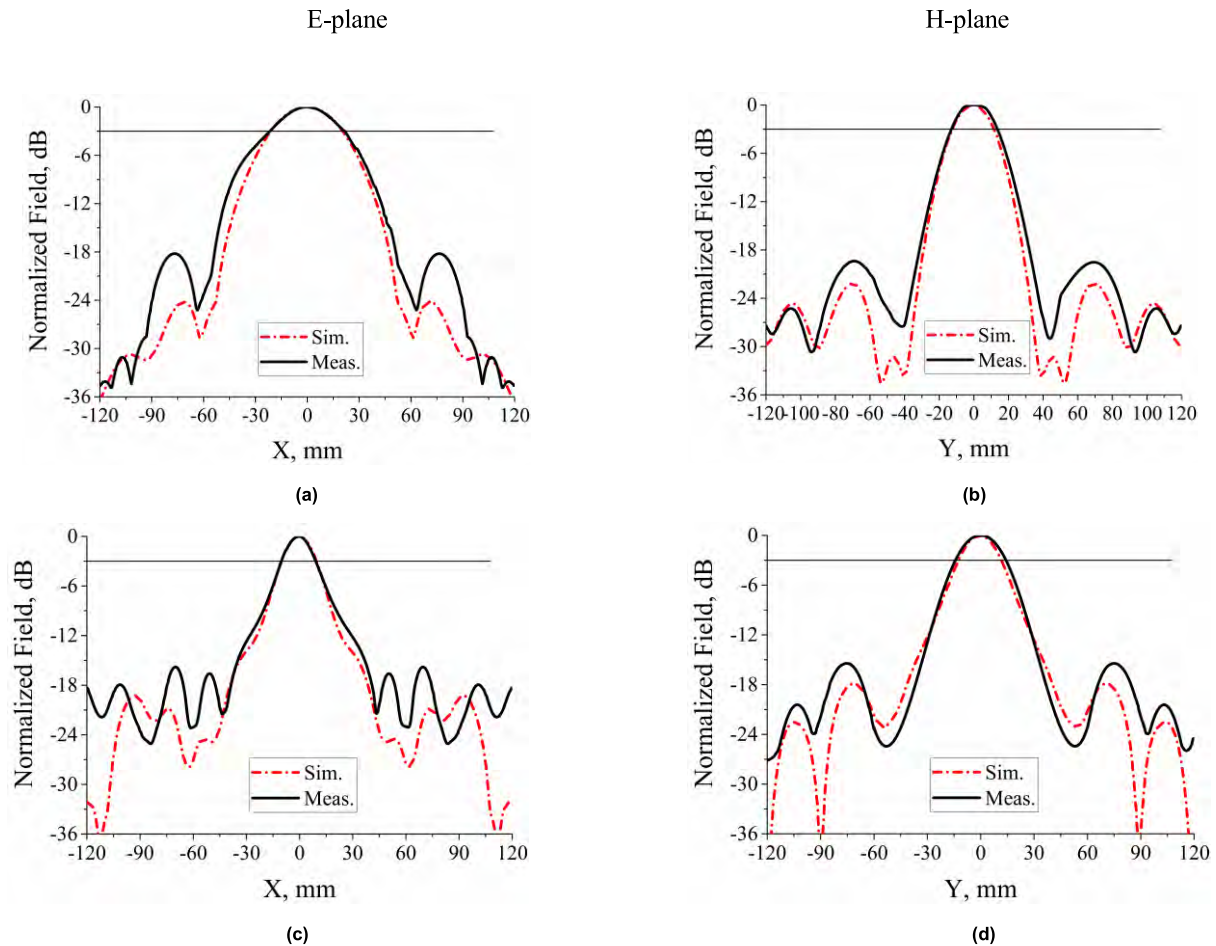


FIGURE 14. Simulated and measured electric field strength distribution of focal plane in E-plane at frequencies of (a) 12GHz, (c) 18 GHz, and in H-plane at frequencies of (b) 12GHz, (d) 18 GHz.

TABLE 3. Bandwidth performance in the lower frequency band.

Frequency (GHz)	Focal Spot Diameter (mm)	
	E-Plane	H-Plane
11.7	63.9	42.6
11.8	53.8	38.7
11.9	45.8	35.2
12.0	43.4	27.0
12.1	50.4	33.6
12.2	59.7	37.8
12.3	71.9	43.6

By comparison, the SD of the E plane is much larger than that of the H plane at 12 GHz, which results in an elliptical focal spot and the average SDs of the measurement is 35.2mm ($1.41\lambda_{\text{lower}}$) at 12GHz and 24.5mm ($1.47\lambda_{\text{higher}}$) at 18GHz. In general, the proposed antenna has excellent focused electromagnetic wave performance and it can meet the requirements of microwave measurement.

The bandwidth performance is presented in Tables 3 and 4, respectively. It is generally believed that when the average SD is less than two wavelengths, the antenna has better focused

TABLE 4. Bandwidth performance in the higher frequency band.

Frequency (GHz)	Focal Spot Diameter (mm)	
	E-Plane	H-Plane
17.7	30.4	39.6
17.8	27.2	38.1
17.9	23.8	33.5
18.0	20.0	29.0
18.1	24.6	37.1
18.2	26.7	42.6

electromagnetic wave [2]. In the low frequency band, the average SD is less than two wavelengths in the range of 11.8-12.2GHz, so the bandwidth is from 11.8 to 12.2GHz. Similarly, in the high frequency band, the bandwidth is from 17.8GHz to 18.1GHz.

Various characteristics of antennas along with the proposed one are tabulated in Table 5 for comparison, where λ_0 is the free space wavelength at the center frequency and λ_m is the average of both free space wavelengths at the center frequencies. It can be seen that the proposed antenna has advantages of good ability to focus electromagnetic wave in the dual-band, which is impossible for the compared antenna.

TABLE 5. Various characteristics of antennas compared with the proposed one.

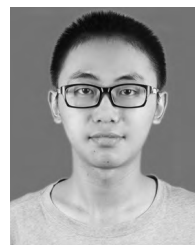
Ref.	Operate Frequency (GHz)	SD	Array Size	Dielectric Substrate
[6]	10	$0.88 \lambda_0$	$51.8 \lambda_0^2$	With
[14]	9.3	$0.88 \lambda_0$	$34.9 \lambda_0^2$	Without
[18]	11/12.5	-	$58.4 \lambda_m^2$	Without
[19]	12/18	-	$132.7 \lambda_m^2$	Without
Proposed antenna	12/18	$1.41 \lambda_{\text{lower}}$ $/1.47 \lambda_{\text{higher}}$	$144 \lambda_m^2$	Without

IV. CONCLUSION

In this paper, a dual-band focused transmitarray antenna using all-metal slot elements is presented. The designed transmitarray antenna consists of a quad-layer metallic array and a pyramidal horn. A 360° transmission phase response can be obtained by changing the length of the I-shaped slot and the L-shaped slots respectively in both low and high frequency bands. The maximum electric field strength is obtained at a point with $6.47 \lambda_{\text{lower}}$ distance from the array aperture at 12 GHz and at a point with $9.78 \lambda_{\text{higher}}$ distance from the array aperture at 18 GHz. Besides, through reasonably arranging the all-metal slot elements, the average SDs of approximately 35.2mm ($1.41 \lambda_{\text{lower}}$) at 12GHz and 24.5mm ($1.47 \lambda_{\text{higher}}$) at 18GHz can be achieved and the dual-band focused transmitarray antenna can operate in two frequency bands 11.8-12.2 and 17.8-18.1 GHz. Compared with the traditional transmitarray antenna, the proposed antenna has advantages of good ability to focus electromagnetic wave in the dual-band, high resistant of poor measurement environment and easy to process. So, it is promising for practical applications of various microwave measurement systems.

REFERENCES

- [1] J. C. Richard and H. Jasik, *Antenna Engineering Handbook*, 4th ed. New York, NY, USA: Wiley, 2007, pp. 648–649.
- [2] T. Jianming, Z. Qing, Z. Ling, L. Shuzhang, and L. Xiangang, "Theory and simulation of 3 mm conical horn focusing lens antennas," *High Power Laser Part. Beams*, vol. 24, no. 2, pp. 436–440, Feb. 2012.
- [3] D. Wu, Z. Feng, and X. Zhuang, "A novel focusing lens conical horn antenna loaded with dielectric," in *Proc. IEEE Int. Wireless Symp. (IWS)*, Shenzhen, China, Mar. 2015, pp. 1–4.
- [4] Z. X. Wang and W. B. Dou, "Dielectric lens antennas designed for millimeter wave application," in *Proc. Joint 31st Int. Conf. Infr. Millim. Waves 14th Int. Conf. Terahertz Electron.*, Shenzhen, China, Sep. 2006, p. 376.
- [5] B. Panzner, A. Joestingmeier, and A. Omar, "Ka-band dielectric lens antenna for resolution enhancement of a GPR," in *Proc. 8th Int. Symp. Antennas, Propag. EM Theory*, Kunming, China, Nov. 2008, pp. 31–34.
- [6] E. G. Plaza, G. Leon, S. Loredó, A. Arboleya, and F. L. Heras, "An ultrathin 2-bit near-field transmitarray lens," *IEEE Antennas Wireless Propag. Lett.*, vol. 16, pp. 1784–1787, 2017.
- [7] A. H. Abdelrahman, A. Z. Elsherbeni, and F. Yang, "Transmitarray antenna design using cross-slot elements with no dielectric substrate," *IEEE Antennas Wireless Propag. Lett.*, vol. 13, pp. 177–180, 2014.
- [8] B. Rahmati and H. R. Hassani, "High-efficient wideband slot transmitarray antenna," *IEEE Trans. Antennas Propag.*, vol. 63, no. 11, pp. 5149–5155, Nov. 2015.
- [9] A. H. Abdelrahman, A. Z. Elsherbeni, and F. Yang, "High-gain and broadband transmitarray antenna using triple-layer spiral dipole elements," *IEEE Antennas Wireless Propag. Lett.*, vol. 13, pp. 1288–1291, Jul. 2014.
- [10] J. Yu, L. Chen, and X. Shi, "A multilayer dipole-type element for circularly polarized transmitarray applications," *IEEE Antennas Wireless Propag. Lett.*, vol. 15, pp. 1877–1880, Dec. 2016.
- [11] C.-Y. Hsu, L.-T. Hwang, P.-S. Lee, S.-M. Wang, and F.-S. Chang, "Design of a high gain and dual polarized transmitarray using FSS of smaller unit cells," in *Proc. Int. Symp. Antennas Propag. (ISAP)*, Okinawa, Japan, Oct. 2016, pp. 776–777.
- [12] Q. Luo, S. Gao, M. Sobhy, and X. Yang, "Wideband transmitarray with reduced profile," *IEEE Antennas Wireless Propag. Lett.*, vol. 17, no. 3, pp. 450–453, Mar. 2018.
- [13] Y. Hou, X. Liu, Y. Li, Z. Zhang, and Z. Feng, "Circular polarization transmitarray element with linear polarization feed," in *Proc. IEEE Int. Conf. Microw. Millim. Wave Technol. (ICMMT)*, Beijing, China, Jun. 2016, pp. 774–776.
- [14] Z. Zhang, X. Li, H. Huang, W. Ouyang, C. Zhao, and C. Sun, "Focused transmitarray antenna using I-shaped slot elements for microwave measurements," *Electron. Lett.*, vol. 25, pp. 1322–1323, Dec. 2019.
- [15] Y. Chen, L. Chen, H. Wang, X.-T. Gu, and X.-W. Shi, "Dual-band crossed-dipole reflectarray with dual-band frequency selective surface," *IEEE Antennas Wireless Propag. Lett.*, vol. 12, pp. 1157–1160, Sep. 2013.
- [16] T. Su, X. Yi, and B. Wu, "X/Ku dual-band single-layer reflectarray antenna," *IEEE Antennas Wireless Propag. Lett.*, vol. 18, no. 2, pp. 338–342, Feb. 2019.
- [17] T. Smith, U. Gothelf, O. S. Kim, and O. Breinbjerg, "Design, manufacturing, and testing of a 20/30-GHz dual-band circularly polarized reflectarray antenna," *IEEE Antennas Wireless Propag. Lett.*, vol. 12, pp. 1480–1483, Nov. 2013.
- [18] M. O. Bagheri, H. R. Hassani, and B. Rahmati, "Dual-band, dual-polarised metallic slot transmitarray antenna," *IET Microw., Antennas Propag.*, vol. 11, no. 3, pp. 402–409, Feb. 2017.
- [19] R. Y. Wu, Y. B. Li, W. Wu, C. B. Shi, and T. J. Cui, "High-gain dual-band transmitarray," *IEEE Trans. Antennas Propag.*, vol. 65, no. 7, pp. 3481–3488, Jul. 2017.
- [20] A. Aziz, F. Yang, S. Xu, and M. Li, "An efficient dual-band orthogonally polarized transmitarray design using three-dipole elements," *IEEE Antennas Wireless Propag. Lett.*, vol. 17, no. 2, pp. 319–322, Feb. 2018.
- [21] K. T. Pham, R. Sauleau, E. Fourn, F. Diaby, A. Clemente, and L. Dussopt, "Dual-band transmitarrays with dual-linear polarization at Ka-band," *IEEE Trans. Antennas Propag.*, vol. 65, no. 12, pp. 7009–7018, Dec. 2017.
- [22] H. Hasani, J. S. Silva, S. Capdevila, M. Garcia-Vigueras, and J. R. Mosig, "Dual-band circularly polarized transmitarray antenna for satellite communications at (20, 30) GHz," *IEEE Trans. Antennas Propag.*, vol. 67, no. 8, pp. 5325–5333, Aug. 2019.



ZHENG ZHANG was born in Henan, China, in 1992. He received the B.S. degree from Zhengzhou University, Henan, in 2015. He is currently pursuing the Ph.D. degree with Xidian University, Xi'an, China. His research interests include frequency selective structures, transmitarray antenna, spot focusing lens, array antenna, and microstrip antennas.



XIAOPING LI was born in Shaanxi, China, in 1961. She received the B.S., M.S., and Ph.D. degrees from Xidian University, Xi'an, China, in 1982, 1988, and 2004, respectively. She is currently a Full Professor with the School of Aerospace Science and Technology, Xidian University. Her current research interests include the near-space vehicle's telemetry tracking and command and communication technology.



CHAO SUN received the B.Eng. and Ph.D. degrees in electromagnetics from Xidian University, Xi'an, China, in 2011 and 2016, respectively. He is currently a Lecturer with the School of Aerospace Science and Technology, Xidian University. His research interests include miniaturization of microstrip antenna, and wideband microstrip antenna.



GAO HAN received the B.S. and M.S. degrees from Xidian University, Xi'an, China, in 2005 and 2012, respectively, where he is currently pursuing the Ph.D. degree with the School of Aerospace Science and Technology. His current research interests include the antenna and wireless power transfer.

...



YANMING LIU received the B.S., M.S., and Ph.D. degrees from Xidian University, Xi'an, China, in 1982, 1988, and 2004, respectively. He is currently a Full Professor with the School of Aerospace Science and Technology, Xidian University. His current research interests include the near-space vehicle's TT and C and communication technology.